Supporting Information

Substrate Coupling Strength of Integrin-Binding Ligands Modulates Adhesion, Spreading, and Differentiation of Human Mesenchymal Stem Cells

Chun Kit K. Choi,[†] Yang J. Xu,[†] Ben Wang,[†] Meiling Zhu,[†] Li Zhang,[†] and Liming Bian[*,†,‡]

[†]Department of Mechanical and Automation Engineering, [‡]Shun Hing Institute of Advanced Engineering, The Chinese University of Hong Kong, Shatin, New Territories, Hong Kong, China

[*]To whom correspondence should be addressed. E-mail: lbian@mae.cuhk.edu.hk.

Table of Contents

Materials

Hydrogen tetrachloroaurate hydrate (Au≥ 48%, $HAuCl_4 \cdot 4H_2O$), trisodium citrate dehydrate (≥ 99%, $C_6H_5Na_3O_7 \cdot 2H_2O$), (3-aminopropyl) triethoxysilane (99%, APTES), and (3-mercaptopropyl) trimethoxysilane (95%, MPTMS) were purchased from Sigma Aldrich (St. Louis, MO) and used without further purification. Acids, hydrogen peroxide (30%, w/w), and ethanol (≥ 99%) were purchased from Thermo Fisher Scientific (Rockford, IL). Cell line human mesenchymal stem cells (hMSCs) were brought from Lonza (Allendale, NJ). Alpha minimum essential medium (α-MEM) and DPBS for cell culture were purchased from Life Technologies (Carlsbad, CA). 4,6-diamidino-2-phenylindole (DAPI) for nuclei staining and chemicals for alkaline phosphatase (ALP) staining were purchased from Sigma Aldrich (St. Louis, MO). Rhodamine phalloidin for the visualization of cytoskeleton was purchased from Life Technologies (Carlsbad, CA). Antibodies used for immunostaining of vinculin and RUNX2 were purchased from Santa Cruz Biotechnology (Dallas, Texas). Bovine serum albumin (BSA) used for surface blocking was purchased from Sigma Aldrich (St. Louis, MO). Thiolated integrin-binding RGD ligand (with the full sequence of GCGYGRGDSPG) containing a cysteine residue at the C-terminus (M.W.: 1025.06) was purchased from GenScript (Piscataway, NJ) and used without further purification. 18 x 18 mm glass coverslips were purchased from Fisher Chemical & Scientific (Pittsburgh, PA). Deionized water with a resistivity of 18.2 MΩ was obtained from a Nanopure water purification system. For nanoparticle synthesis, all the necessary glassware was thoroughly cleaned with fresh aqua regia solution (HCl/HNO_3, 3:1, v/v) prior to the experiment.

Methods

1. Preparation and Characterization of Citrate-Capped Gold Nanoparticles (Cit-AuNPs)

Citrate-capped gold nanoparticles (cit-AuNPs) of ~50 nm in diameter were synthesized as previously reported.[1] 50 mL of deionized water was allowed to boil under reflux. 1.214 mL of 10 mM $HAuCl_4$ (aq) was injected, followed by the addition of 0.5 mL of 10 mg/mL citrate (aq). Upon vigorous stirring for 1 min, color change from dark blue to wine red was observed. The mixture was further refluxed for 30 min and allowed to cool down to room temperature. The cit-AuNP solution was collected in glass vial and used throughout the study.

UV-vis spectrum of the cit-AuNP solution was obtained using a UV-vis spectrophotometer (Cary 5000, Agilent, USA). 1-cm-path length quartz cuvette was used to contain the sample and all spectra were collected within the range of 400–800

nm. Dynamic light scattering (DLS) measurement was performed at room temperature using NanoSight (NS500, Thermo Fisher Scientific, USA). Zeta potential measurement was performed at room temperature on a zeta potential analyzer (ZetaPlus, Brookhaven Instruments Co., USA). Samples were diluted to obtain stable signals and ten measurements were performed to give the data presented as mean ± sd. 0.5 μL of the cit-AuNPs stock solution was dipped onto 400-mesh copper TEM grid (Electron Microscopy Sciences) and then visualized by transmission electron microscopy (TEM, TS12, FEI, USA) operating at 120 kV. For the determination of physical size, over 100 particles were analyzed in multiple TEM images captured from different areas of the TEM grid. The diameter of particles was measured using ImageJ (NIH).

2. Conjugation of the Thiolated-RGD Peptides onto Cit-AuNPs in Buffer

A series of thiolated RGD peptide solutions with different concentrations (i.e., 1, 3, 9, and 12 μM) was prepared by dissolving the powder of peptide in PBS buffer (pH 7.4). 5 mL of the peptide solution was mixed and incubated with 5 mL of the cit-AuNP solution for 2 h. Excess peptides were removed by centrifugation. Subsequently, 2 mL of the product was extracted for UV-vis spectroscopy. The shift of the absorption peak maximum of the resultant solution was monitored.

3. Fabrication of RGD-Coupled Surfaces with Varied Coupling Strength

Low-coupling-strength surfaces (LCS0.5 and LCS12.5) and high-coupling-strength surfaces (HCS25 and HCS50) were fabricated in the same manner except that the dosage of APTES (%, v/v, in ethanol) used for modification was varied, as indicated by their respective name. Briefly, glass coverslips were first rinsed by sonication in deionized water and ethanol for several times to remove organics. Then, surfaces of the cleaned coverslips were activated by acid treatment in piranha solution (H_2SO_4/H_2O_2, 4:1, v/v) for 30 min. This step was repeated once. The treated coverslips (bearing hydroxyl groups) were finally washed in water and then dried under nitrogen stream. In order to decorate the glass substrate with different positive charge densities, the freshly prepared coverslips were then immersed in ethanolic solutions of APTES with varying APTES dosages (i.e., 0.5%, 12.5%, 25%, and 50%) for 2 h. The APTES-modified coverslips were then rinsed successively in water and ethanol, followed by drying in oven at 100 ^{o}C for 1 h. Following that, the as-prepared coverslips were coated with a monolayer of cit-AuNPs through the immersion in cit-AuNP solution for 3 h. The cit-AuNP stock solution was diluted so that the nanoparticles were randomly distributed with similar density among each of the surfaces. Finally, the AuNP-coated coverslips were allowed to conjugate with the thiolated RGD peptides upon the immersion in 9 μM of the thiolated RGD peptide solution (buffered at pH 7.4) at 37 ^{o}C for 2 h prior to the cell experiment.

4. Characterization of the RGD-Coupled Surfaces

The inter-particle spacing of all the RGD-coupled surfaces was qualitatively examined by scanning electron microscopy (SEM, LEO-32, LEO Electron Microscopy Ltd., UK) operating at an accelerating voltage of 10 kV. Before the examination, samples were sputter coated with a thin layer of gold for 30 s in order to acquire better images. At least ten images from different areas of the coverslips were taken for analysis.

The surface chemical composition of the fabricated glass substrates was determined by X-ray photoelectron spectroscopy (XPS, SKL-12 X-ray photoelectron spectrometer, China). Respective X-ray photoelectron spectrum of each of the fabricated surfaces was shown in Figure S2.

Contact angle measurement of the fabricated glass substrates was performed by using a contact angle analyzer (GAOSUO, Cooling Tech 2.0). Briefly, 10 μL of water droplet was pipetted onto the surfaces for image acquisition in which the camera was placed at a fixed angle.

The substrate coupling strength of cit-AuNPs (and thus the RGD peptides) immobilized on the fabricated glass substrates was examined by atomic force microscopy (AFM, BioScope Catalyst, Bruker, Germany) operating in contact mode. The force constant of the AFM cantilever (MSNL-10, Bruker) was kept as 0.6 N/m throughout the study. To obtain the images shown in Figure 2c, we first scanned the surface in contact mode with a scan size of 10 x 10 μm with an increasing deflection setpoint voltage (starting from 1.000 V for all the fabricated surfaces) with a step size of 0.500 V until the surface particles can be scanned off. Following that, we scanned the surface in ScanAsyst mode with a scan size of 40 x 40 μm in order to capture the region of interest of which surface particles were scanned previously. Analysis was conducted in air and at ambient temperature.

5. Cell Culture

All cell experiments associated in this study were conducted at 37 ^{o}C and 5% CO_2. Human mesenchymal stem cells (hMSCs) (Lonza) were expanded to passage 3 in basal medium, i.e., αlpha-Minimum Essential Medium supplemented with 10% FBS (Invitrogen), 1% streptomycin/penicillin (Invitrogen), and 1% L-glutamine (Invitrogen). Following that, hMSCs were seeded at a constant density of 5 000 cells/cm^2 onto the RGD-coupled surfaces (or control surfaces) and incubated for 1 day or 3 days before the fixation. All cell culture and subsequent staining were performed in a 6-well plate.

For differentiation assay, HMSCs were cultured in osteogenic induction medium (i.e., basal medium added with 10 mM bone morphogenetic protein (Invitrogen), 50 μg/mL L-ascorbic acid 2-phosphate (Sigma Aldrich), and 100 nM dexamethasone

(Sigma Aldrich) for 7 days following 1 day of adhesion in basal medium.

6. Fluorescence and Immunofluorescence Labeling

Briefly, hMSCs were fixed with 4% formalin for 15 min at room temperature, rinsed with DPBS (Invitrogen) for three times, permeabilized with 2% triton-X 100 (Sigma Aldrich) in DPBS for 10 min at room temperature, and then blocked with 1% bovine serum albumin (BSA) (Sigma Aldrich) at 37 ^{o}C for 1 h. To visualize F-actin stress fibers, hMSCs were stained with 1:200 rhodamine phalloidin (Life Technologies) in 0.5% BSA in PBS for 1 h in dark and counter-stained for nuclei with 1:1000 DAPI in PBS for 20 min.

For osteogenic differentiation study, cells were immuno-stained with 1:100 primary antibodies (Santa Cruz Biotechnology, sc–101145) against RUNX2 or 1:100 primary antibodies against YAP (Santa Cruz Biotechnology, sc–15407) in 0.5% BSA in PBS for overnight at 4 ^{o}C. Secondary antibody labeling was performed by incubation in 1:200 labeled goat anti-mouse or anti-rabbit IgG (Life Technologies, A-11001) containing Alexa488-phalloidin in 0.5% BSA in PBS for 2 h at room temperature.

7. ALP Staining

hMSCs allowed to differentiate in osteogenic induction medium for 7 days were stained for alkaline phosphatase (ALP). Briefly, hMSCs were fixed in 4% formalin for 15 min at room temperature, rinsed with PBS, and then incubated in the staining solution containing 4% of naphthol AS-MX phosphate (Sigma Aldrich) in Fast Blue RR Salt solution (Sigma Aldrich) in deionized water for 20 min at room temperature in dark. Next, hMSCs were rinsed in PBS and imaged under a microscope with a constant illumination.

8. Fluorescence Microscopy

hMSCs on the coverslips were imaged under a Nikon Eclipse TI microscope (Nikon). In the whole study, cell images were taken using the same exposure settings for analysis. Regarding the examination of intensity of both the early osteogenesis marker RUNX2 and the transcriptional regulator YAP, the nuclear fluorescence of cells was determined by drawing a region of interest in ImageJ (NIH) around the nuclei and the average cytoplasmic fluorescence for each cell was subtracted from this value to determine the relative fluorescence intensity.

9. Image Analysis and Statistics

In the whole study, cell images were analyzed using Image J (NIH). For the quantification of morphological characteristics, over 100 cells in multiple images taken on different areas of the same sample were analyzed. For the differentiation study, the scatter diagram shown in Figure S11a was plotted by calculating the ratio of RUNX2 nuclear to cytoplasmic mean fluorescent intensity. Over 50 cells captured in

multiple images of the same sample were analyzed. The percentage of RUNX2 positive cells was determined by counting cells that display the green nuclear fluorescence. Following that, the value was compared to total nuclei count using DAPI. Over 500 cells captured in multiple images of the same sample were examined to obtain the plot in Figure S11b. Similarly, the scatter diagram shown in Figure S12 was plotted by calculating the ratio of YAP nuclear to cytoplasmic mean fluorescent intensity. Over 25 cells captured in multiple images of the same sample were analyzed.

For statistical analyses, 2-way ANOVAs were performed on all the collected data as presented in this study.

Figure S1

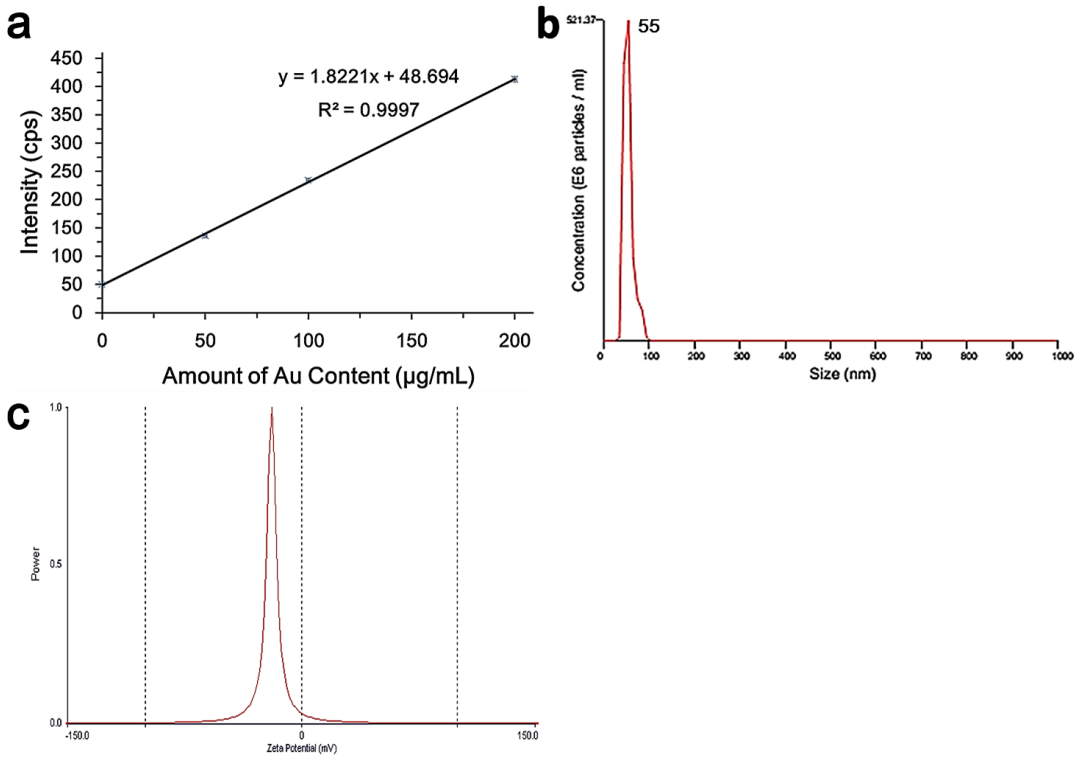

Figure S1. Characterization of the synthesized citrate-capped gold nanoparticles (cit-AuNPs). (a) Standard linear calibration curve obtained from the inductively coupled plasma optical emission spectrometry (ICP-OES) of varying concentrations of gold standard solutions. This calibration curve is used to determine the concentration of the stock solution of cit-AuNPs. Data obtained from three independent measurements are presented as mean ± SD. (b) Dynamic light scattering (DLS) measurement of the cit-AuNPs in water at 25 ^{o}C. (c) Zeta potential measurement of the cit-AuNPs in water at 25 ^{o}C.

Figure S2

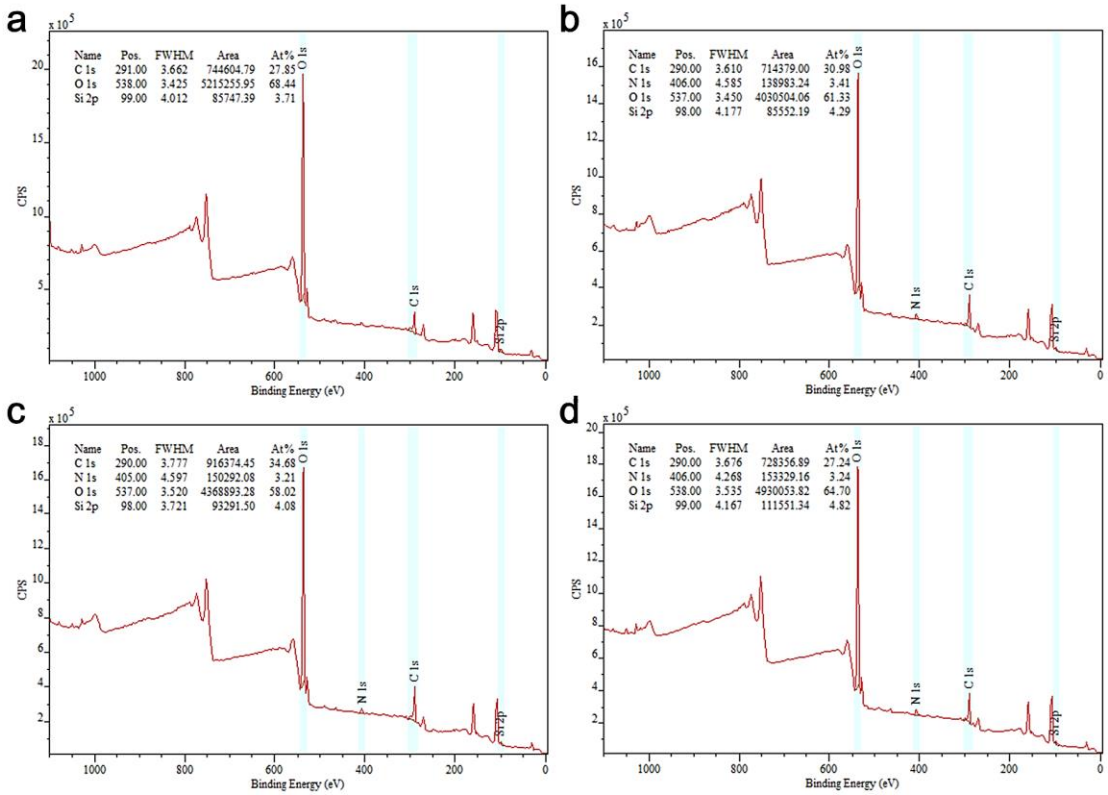

Figure S2. X-ray photoelectron spectroscopy (XPS) of the RGD-coupled surfaces named as (a) LCS0.5, (b) LCS12.5, (c) HCS25, and (d) HCS50. All XPS spectra are obtained prior to the conjugation of the RGD peptides. Analysis of the surface chemical composition of the fabricated surfaces shows a slight but gradual increase in the portion of nitrogen atoms on the surfaces with increasing coupling strength, indicating the difference in the surface density of APTES molecules on the fabricated surfaces modified with different dosages of APTES.

Figure S3

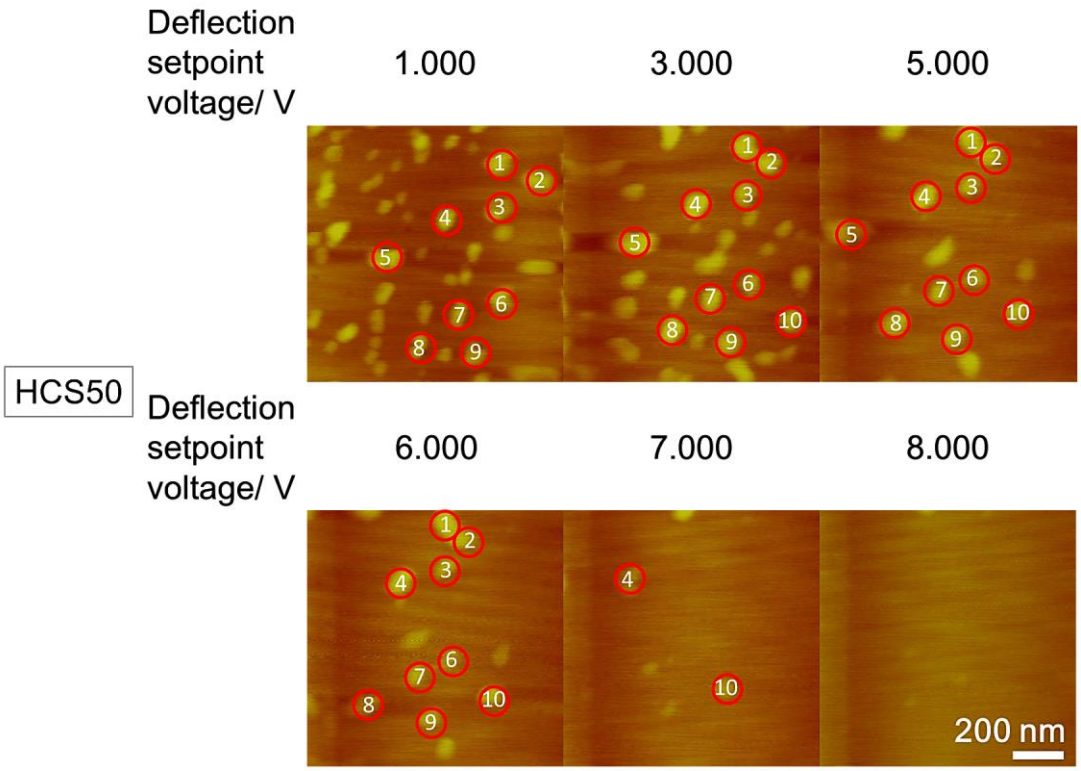

Figure S3. Examination of the substrate coupling strength of immobilized cit-AuNPs on high-coupling-strength surface (HCS50) by atomic force microscopy (AFM) operating in contact mode. Our results show that all the particles immobilized on HCS50 can be swiped away by the AFM cantilever until the deflection setpoint voltage reaches 8.000 V. Scale bar is 200 nm.

Figure S4

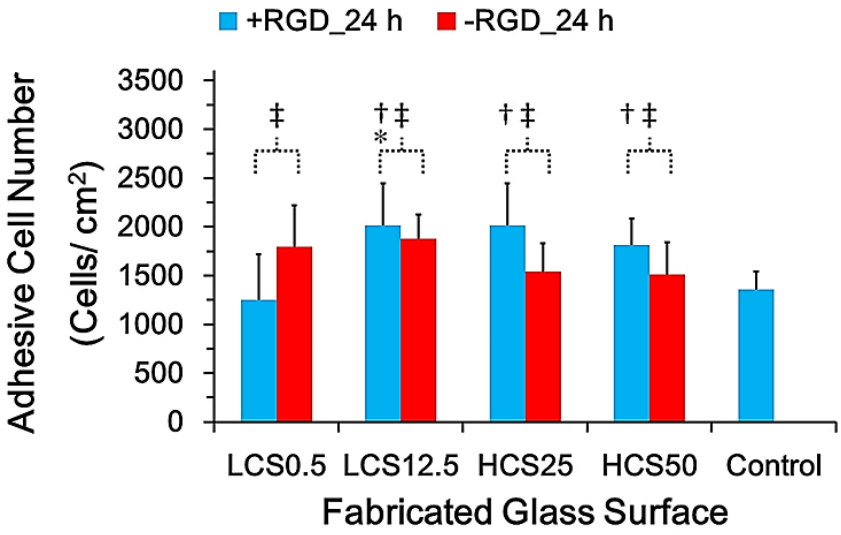

Figure S4. Statistical results of the cell adhesive property of the RGD-coupled surfaces. hMSCs are grown on the surfaces for 24 h. Over 10 multiple fluorescence images are obtained under a 4× magnification and analyzed for the number of adherent cells. Data are presented as mean ± sd. *, significant statistical difference compared to other experimental groups ($p<0.01$); †, significant statistical difference compared to the blank control surface ($p<0.05$); ‡, significant statistical difference compared to the negative control ($p<0.01$).

Figure S5

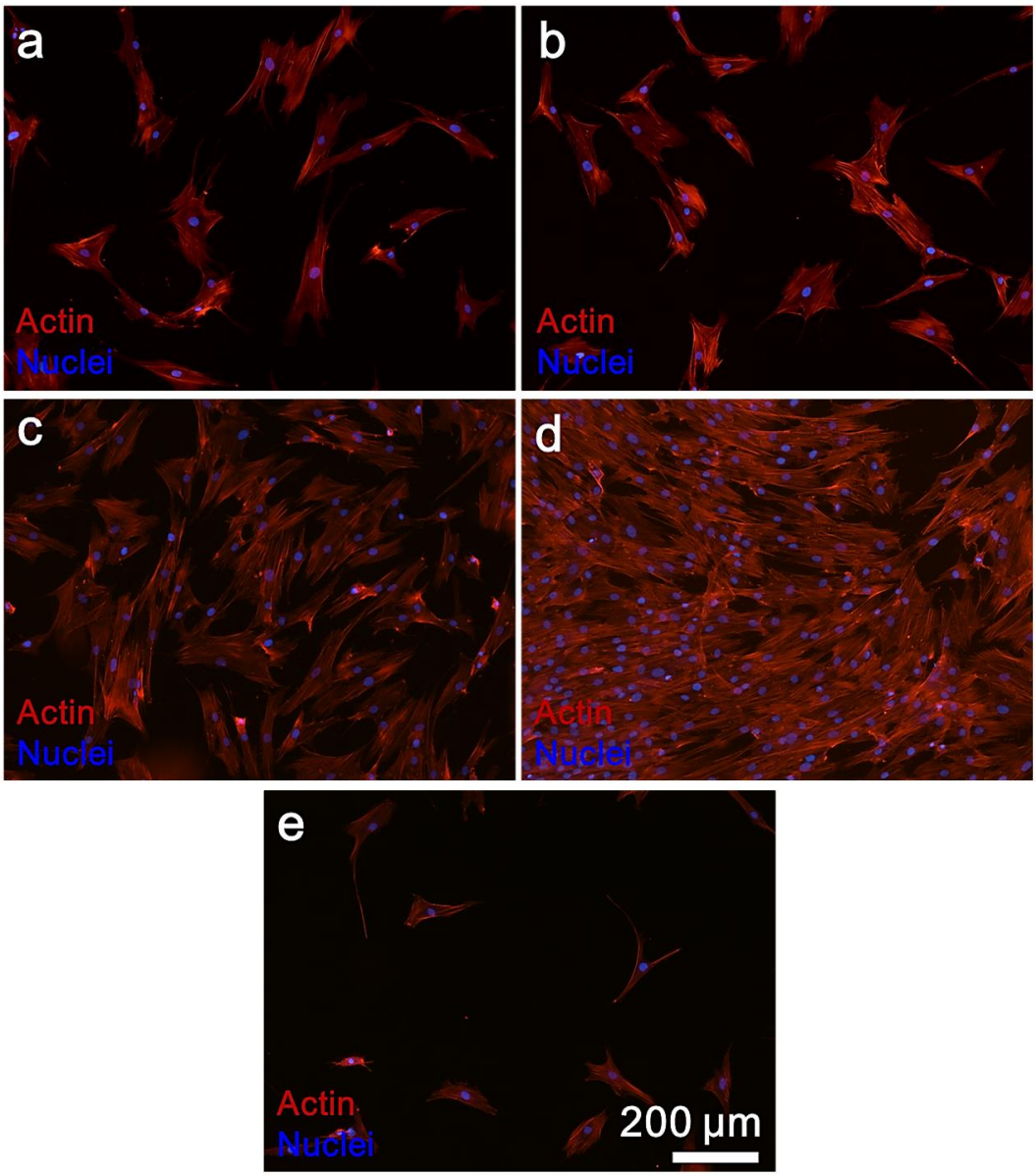

Figure S5. Representative fluorescence micrographs of the hMSCs cultured on the negative control surfaces with (a) 0.5%, (b) 12.5%, (c) 25%, and (d) 50% of APTES modification only but without any nanoparticle immobilization. Result for the blank control surface is shown in (e) for comparison. Cells are grown on the control surfaces for 24 h. We observe in at least two independent experiments that a significantly higher number of adherent cells are present on all the APTES-treated surfaces compared to that on the blank control surface. More importantly, hMSCs spread well when grown on surfaces with a higher degree of APTES modification, indicating the difference in positive charge density among each of the surfaces. Scale bar is 200 μm.

Figure S6

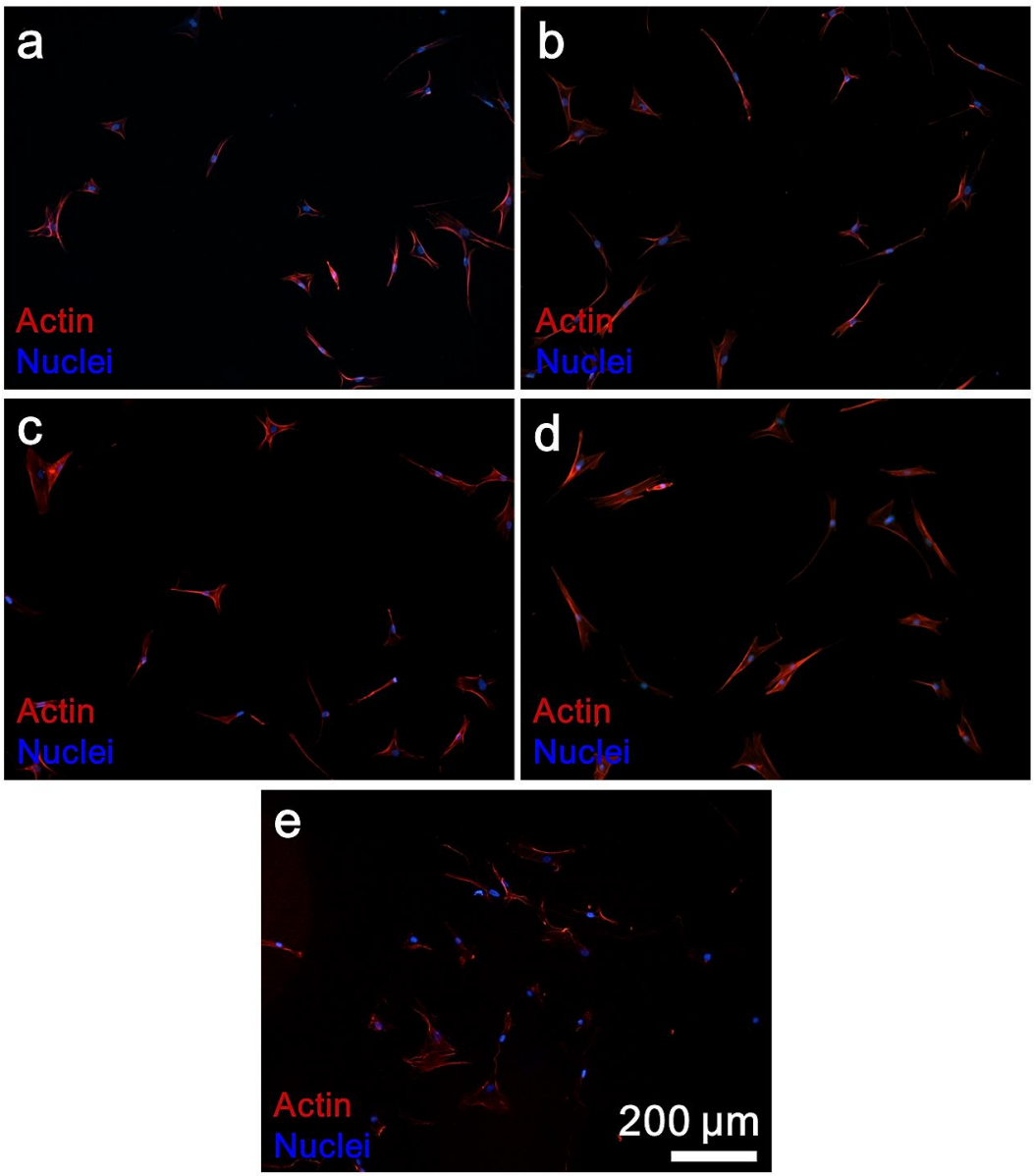

Figure S6. Representative fluorescence micrographs of the hMSCs cultured on the negative control surfaces with (a) 0.5%, (b) 12.5%, (c) 25%, and (d) 50% of APTES modification and cit-AuNP immobilization only but without the conjugation of the RGD peptides. Result for the blank control surface is shown in (e) for comparison. Cells are grown on the control surfaces for 24 h. There is no observable difference in adherent cell numbers among each of the surfaces. More importantly, in the absence of RGD, hMSCs appear similarly in morphology as spindle-like without significant spreading, regardless of the degree of APTES modification. These results indicate that the monolayer of cit-AuNPs masks the positive charge effect on stem cell behaviors as observed previously in Figure S5. Scale bar is 200 μm.

Figure S7

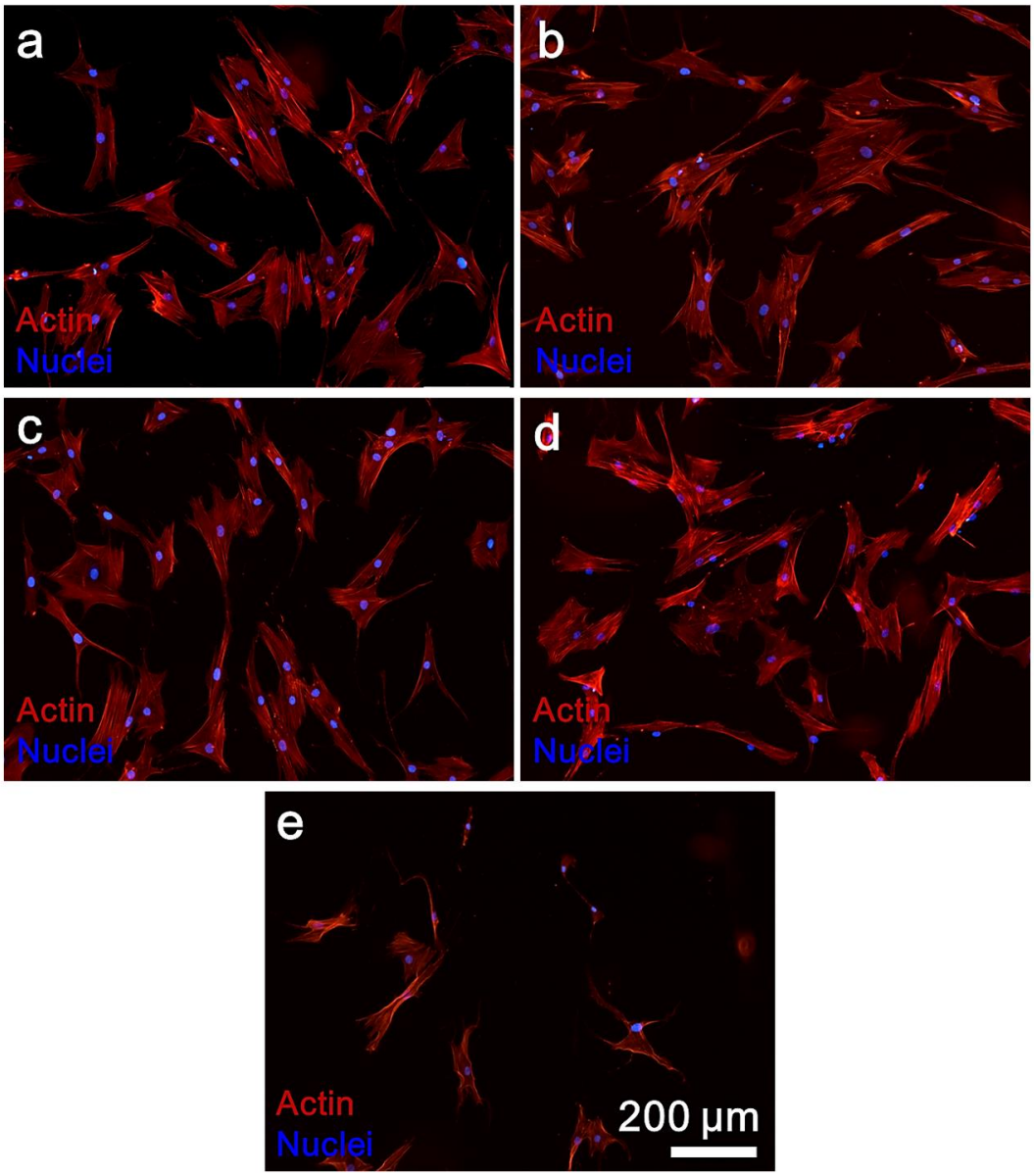

Figure S7. Representative fluorescence micrographs of the hMSCs cultured on the positive control surfaces with (a) 0.5%, (b) 12.5%, (c) 25%, and (d) 50% of MPTMS modification. Result for the blank control surface is shown in (e) for comparison. Cit-AuNPs are covalently attached onto the glass substrate via the S–Au bond instead of electrostatic interactions, followed by the conjugation of the RGD peptides. Cells are grown on the control surfaces for 24 h. There is no observable difference in adherent cell numbers, morphology, and spreading of hMSCs among each of the surfaces. These results support our claim that varying the coupling strength of the RGD peptide on the substrate can modulate adhesion as well as spreading of hMSCs. Scale bar is 200 μm.

Figure S8

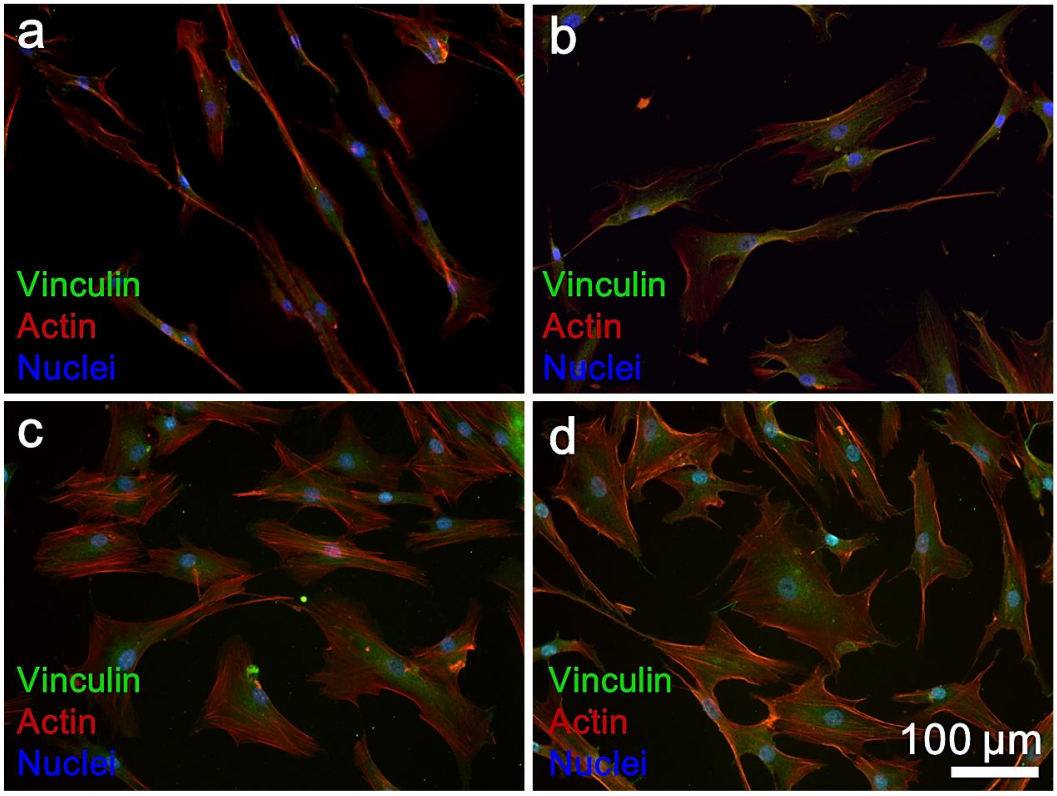

Figure S8. Low-magnification fluorescence micrographs of the hMSCs cultured on (a) LCS0.5, (b) LCS12.5, (c) HCS25, and (d) HCS50 for 3 days. We observe a global effect on the differential responses in stem cell morphology but not a localized effect among a cell population grown on the fabricated surfaces. Scale bar is 100 μm.

Figure S9

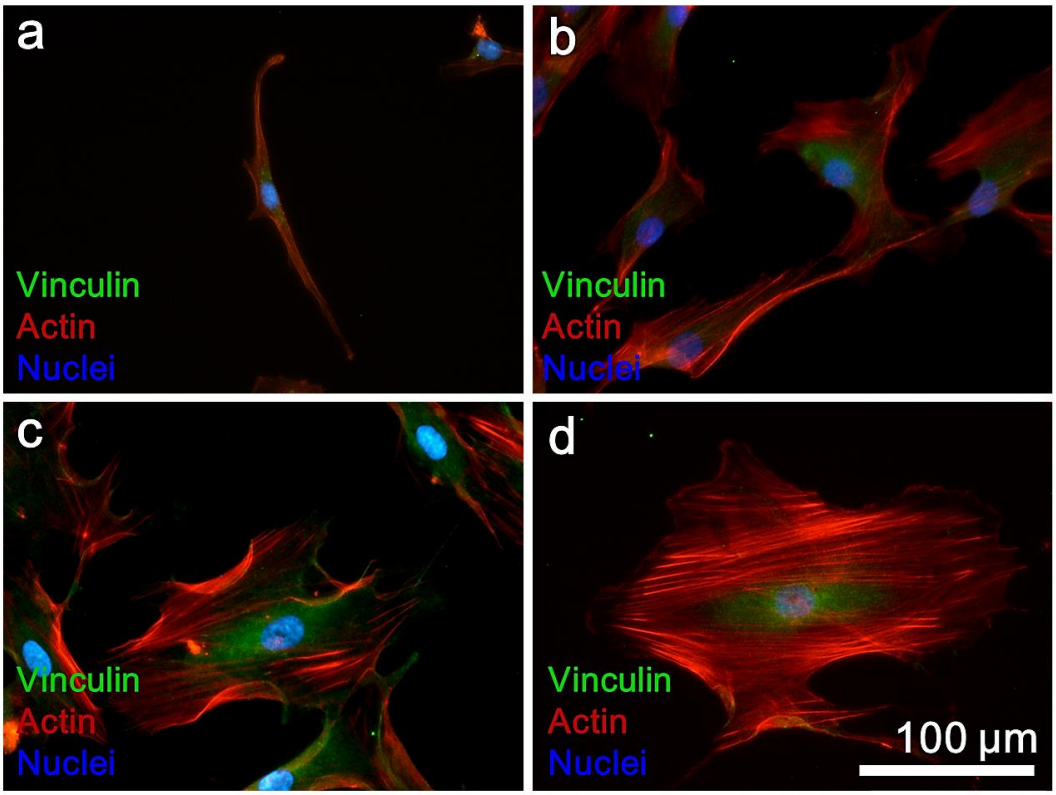

Figure S9. High-magnification fluorescence micrographs of the hMSCs cultured on (a) LCS0.5, (b) LCS12.5, (c) HCS25, and (d) HCS50 for 3 days. There is a lack of formation of well-defined actin fibers for hMSCs grown on LCS surfaces. In contrast, cells on HCS surfaces produce prominent, ordered, and continuous actin filaments that span over the whole cytoplasm, especially for cells on HCS50. Scale bar is 100 μm.

Figure S10

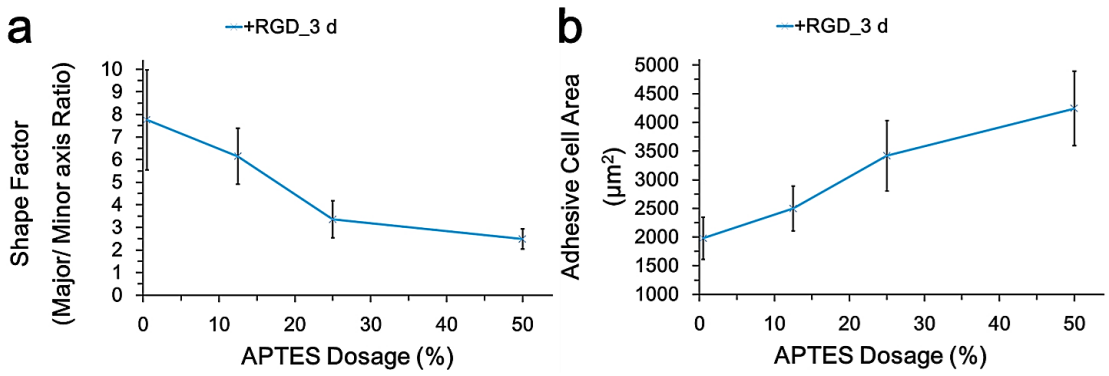

Figure S10. Statistical results of the structural responses of the hMSCs cultured on the RGD-coupled surfaces for 3 days. (a), (b) Plot of shape factor and adhesive cell area as a function of APTES dosage, respectively. There is a decreasing trend of the aspect ratio when cells are grown on the surfaces with increasing substrate coupling strength of the RGD peptides. Conversely, the cell spread area is monotonically increasing with the substrate coupling strength of the RGD peptides.

Figure S11

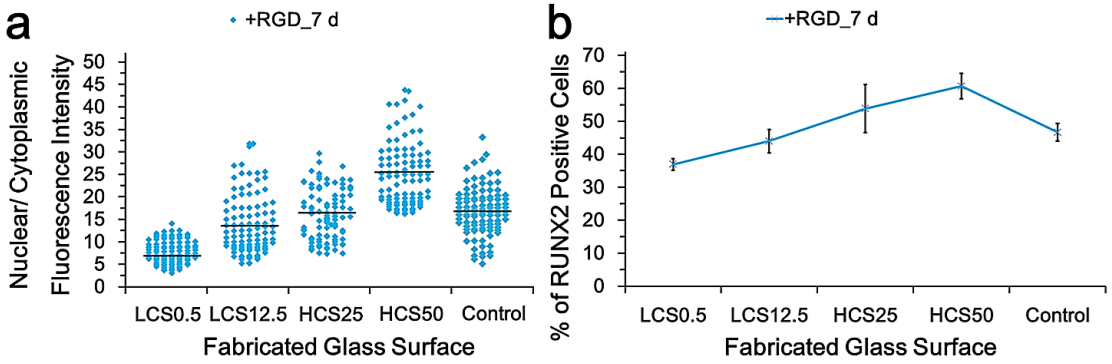

Figure S11. Statistical results of RUNX2 staining of the hMSCs differentiated on the RGD-coupled surfaces for 7 days. (a) RUNX2 nuclear to cytoplasmic mean fluorescence intensity ratio is plotted as a scatter diagram for cells undergone osteogenic differentiation on each surface. Over 50 cells are analyzed to obtain the data in which the black line represents the mean value. hMSCs cultured on HCS surfaces exhibit a relatively higher RUNX2 nuclear to cytoplasmic mean fluorescence intensity ratio than cells cultured on LCS surfaces. (b) Percentage of RUNX2 positive cells is obtained for the same cell sample differentiated on each of the surfaces. An increasing population of hMSCs shows positive RUNX2 staining when differentiated on surfaces with increasing coupling strength of the RGD peptide.

Figure S12

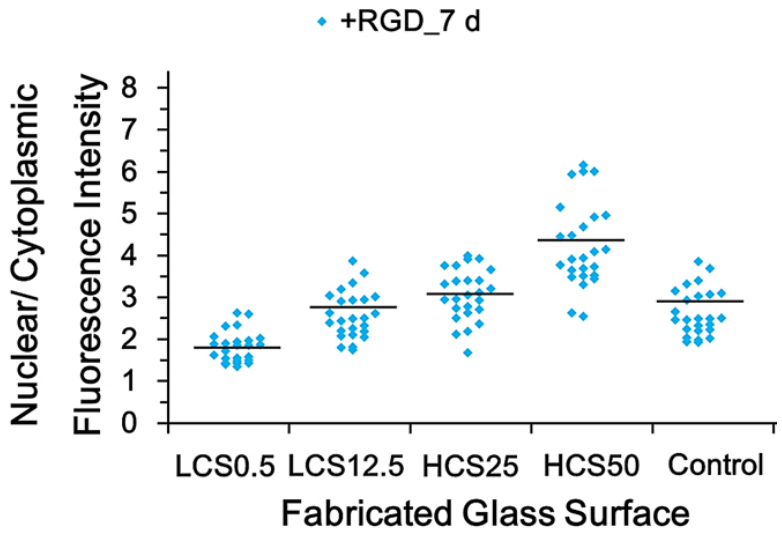

Figure S12. Statistical results of YAP staining of the hMSCs differentiated on the RGD-coupled surfaces for 7 days. YAP nuclear to cytoplasmic mean fluorescence intensity ratio is plotted as a scatter diagram for cells undergone osteogenic differentiation on each surface. Over 25 cells are analyzed to obtain the data in which the black line represents the mean value. hMSCs cultured on HCS surfaces exhibit a relatively higher YAP nuclear to cytoplasmic mean fluorescence intensity ratio than that on LCS surfaces show.

References

1. Grabar, K. C.; Brown, K. R.; Keating, C. D.; Stranick, S. J.; Tang, S. L.; Natan, M. J. *Anal. Chem.* **1997,** 69, 471–477.